Free Vibration Analysis of Twisted Functionally Graded Material Plates

Thesis submitted in partial fulfillment of the requirements for the degree of

Master of Technology

in

Civil Engineering

(Specialization: Structural Engineering)

by

PRATHEESH P P

212CE2037

Department of Civil Engineering
National Institute of Technology Rourkela
Rourkela, Odisha, 769008, India
May 2014

Free Vibration Analysis of Twisted Functionally Graded Material Plates

Dissertation submitted in

May 2014

to the department of

Civil Engineering

of

National Institute of Technology Rourkela

in partial fulfillment of the requirements for the degree of

Master of Technology

by

PRATHEESH P P

(Roll 212CE2037)

under the supervision of

Prof. A V ASHA

Department of Civil Engineering
National Institute of Technology Rourkela
Rourkela, Odisha, 769008, India

Department of Civil Engineering
National Institute of Technology Rourkela
Rourkela-769008, Odisha, India.

Certificate

This is to certify that the work in the thesis entitled ***Free Vibration Analysis of Twisted Functionally Graded Material Plates*** by ***Pratheesh P P*** is a record of an original research work carried out by him under my supervision and guidance in partial fulfillment of the requirements for the award of the degree of Master of Technology with the specialization of **Structural Engineering** in the department of **Civil Engineering**, National Institute of Technology Rourkela. Neither this thesis nor any part of it has been submitted for any degree or academic award elsewhere.

Place: NIT Rourkela

Date: May 2014

Prof. A V Asha

Civil Engineering Department

NIT Rourkela, Odisha

Acknowledgment

With immense pleasure, I express my sincere gratitude towards my supervisor **Prof. A.V. Asha** for her invaluable guidance and constant inspiration. She encouraged me to remain focused on the project and to move forward with the investigation in depth.

I am greatly thankful to **Prof. N. Roy**, Head of the Department of Civil Engineering for providing all kinds of possible advice and help during the study.

I am extremely thankful to all the staff members of the department and all my well-wishers, classmates and friends for their inspiration and help.

Last, but not the least, I would like to acknowledge the support, love and motivation I received from my parents and my brother.

Place: NIT Rourkela
Date: May 2014

Pratheesh P.P
M. Tech, Roll No: 212CE2037
Structural Engineering
Department of Civil Engineering
NIT Rourkela, Odisha

Abstract

The application and demand for composite materials is expanding nowadays. Composite materials find applications in space antennae, aerospace structures and ship structures. For high temperature applications, the functionally graded material gives good performance compared to the laminated composite materials. The twisted plates have various applications in the power generation field such as generator and turbine blades. Due to light weight and high stiffness properties, the Functionally Graded Materials are economical as they require less power. Many of these plates are subjected to high temperature environment in these applications; hence functionally graded material is a good alternative to metal plates.

The present paper will explore the free vibration behavior of thin twisted functionally graded material (FGM) plates. The vibration analysis is done using finite element method. An 8 noded shell element is used for finite element calculations. To model the FGM section, continuous variation in the material property along the thickness is approximated to a laminated composite section consisting of a number of layers and each layer is considered as isotropic. The material property in each layer is determined using power law. Material density, Young's modulus and Poisson's ratio change along the thickness based on power law. The first order shear deformation theory is used in the analysis of pretwisted FGM plate. Convergence of fundamental frequencies is observed, with an increase in mesh size and the number of layers in the thickness direction. To validate the finite element model, for different boundary conditions, the free vibration results are compared with analytical studies and experimental studies. Having fixed the mesh size and number of layers required to represent the material property variation along the depth, the changes in frequencies with variation in angle of twist and material property index is studied. The effect of geometric variables such as gradient index, aspect ratio, side to thickness ratio and angle of twist on the free vibration of cantilever twisted plates is studied. Temperature dependent material properties

are considered as well as nonlinear material property variation along the thickness due to temperature. The influence of thermal gradient along the thickness direction on the free vibration of cantilever twisted plates is studied.

Contents

List of Figures

List of Tables

List of Abbreviations

a, b   :   Length and width of plate

h   :   Thickness of plate

a/b   :   Aspect ratio

b/h   :   Width to thickness ratio

n   :   Gradient index

ϕ :   Angle of twist of twisted panel

n   :   Gradient index

R_x, R_Y :   Radius of curvature in 'x' and 'y' direction respectively

R_{xy} :   Twist radius

A_{ij} :   Extensional stiffness

B_{ij} :   Coupling stiffness

D_{ij} :   Bending stiffness

S_{ij} :   shear stiffness

$[B]$:   Strain displacement matrix

$[D]$:   Stress strain matrix

E   :   Modulii of elasticity

G   :   Shear modulii

$[J]$:   Jacobian matrix

$[k_e]$:   Element elastic stiffness matrix

$[K_e]$:   Global elastic stiffness matrix

$[K_g]$:   Global initial stress stiffness matrix

$[M]$:   Global mass matrix

$[m_e]$:   Element mass matrix

N_i :   Shape function

$[N]$:   Shape function matrix

$[P]$:   Density parameters

ρ :   Mass density

N_x, N_y, N_{xy}	:	In plane stress resultants
u, v, w	:	Displacement components in x,y and z direction
γ	:	Shear strain
$\epsilon_x, \epsilon_y, \epsilon_{xy}$	:	Linear strain
$\epsilon_{xnl}, \epsilon_{ynl}, \epsilon_{xy}$	:	Non-linear strain
ξ_x, η_y	:	Natural coordinates
$\sigma_x{}^0, \sigma_x{}^0, \sigma_{xy}{}^0$	:	In plane stress in x,y and z direction respectively
$\tau_{xy}{}^0, \tau_{xz}{}^0, \tau_{yz}{}^0$	:	shear stress in xy,xz and yz planes respectively
θ_x, θ_y	:	Rotation of mid surface about x and y respectively
ω	:	frequencies of vibration
Ω	:	Non-dimensional frequency parameter
κ	:	Thermal conductivity
α	:	Thermal expansion coefficient

Chapter 1

INTRODUCTION

Chapter 1

Introduction

1.1 Introduction to FGM

Composite materials are a class of advanced materials made by combining one or more materials in the solid state with distinct chemical and physical properties. These composite materials offer superior properties compared to their parent materials and are also light in weight. FGMs are an advanced class of composite materials with varying material property over the change in dimension. Due to the gradual change in material property from one surface to another, it can eliminate inter laminar stress due to sudden change in material property. The materials and their composition are selected based on the function the material has to perform. Metal ceramic FGMs are commonly used as a thermal barrier material, where the ceramic surface will resist the temperature and the metal matrix will provide the strength. The idea of FGM originated in Japan in 1984 for a space research, in the form of a temperature resistant material that can withstand a temperature of two thousand Kelvin and a thermal gradient of thousand Kelvin with thickness less than ten millimeter. Functionally graded materials can be used in adverse operating conditions such as high temperature and moisture. These materials have applications in rocket heat shields, thermal and sound insulation structural walls, wear-resistant linings, thermoelectric generators, heat exchanger tubes, fusion reactor's thermal lining and electrically insulating metal/ceramic joints. Due to the rising applications of FGM in materials subjected to periodic loading and dynamic forces, it is necessary to study the dynamic behavior of these plates subjected to

temperature and with various boundary conditions.

The structural unit of an FGM can be represented by the material ingredient. It indicates rate at which material properties are varying. The chemical composition, geometric configuration and physical state of FGM depends on the gradient index. Basic FGM consists of a two material mixture in which material composition varies from one point to another. The material properties are also varying stepwise. Change in porosity from one surface to another also create FGM. A gradual increase in the porosity creates thermal resistance, impact resistance and low density.

1.2 Importance of the present study

The functionally graded material twisted plates can be used as turbine blades, and engine blades of jet engines due to their high stiffness and strength to density ratio. The functionally graded material provides good thermal resistance and stability in high thermal environments. These turbine blades and engine components are subjected to dynamic forces so the natural frequency of vibration is a very important design criteria. In the present study, the effect of geometric variables on the natural frequency of cantilever pretwisted plates is studied.

1.3 Outline of the present work

The present work studies the free vibration of FGM twisted plates. The influence of temperature environment on the free vibration behavior is studied. The effect of different variables like twist angle, width to thickness ratio, gradient index and aspect ratio are examined. Thermal effects on the material properties are considered in the analysis.

In the first chapter, introduction about FGM and the necessity of this study is explained.

Chapter 2 consists of a literature review on the previous studies in this field. The purpose and need of the present study is outlined.

In Chapter 3, theoretical formulations for free vibration analysis using finite element method is explained in detail. A MATLAB code based on finite element method is developed to perform necessary computations. The MATLAB code is used to plot the mode shapes.

Chapter 4 consists of convergence study, validation of the formulation and free vibration results of twisted cantilever plates. The studies have been done for functionally graded material twisted plates with different gradient index.

Chapter 5 consists of concluding remarks of the present study and scope of future work.

Chapter 2

LITERATURE REVIEW

Chapter 2

LITERATURE REVIEW

2.1 Literature review

Wetherhold et al. [29] studied the use of functionally graded materials in controlling thermal deformation. By changing the fiber material content within a laminated composite beam and a gradual change in material property, temperature deflections were reduced.

Reddy and Chin [19] presented the vibration of graded cylinder and plate. Finite element formulation developed takes in to account the thermo-mechanical effects. Thermo-mechanical effects have a more dominant effect on the radial stress, compared to the hoop stress in the case of cylinder.

Nabi and Ganesan [14] studied vibration properties of initially twisted composite plates considering plate and beam theory. For the analysis of twisted composite beams, torsion flexure, shear flexure and flexure are considered. Triangular plate element was used to represent the beam to an equivalent plate element. Parametric studies are conducted using plate and beam theories. The parameters considered in the analysis were layer sequence, twisting angle, orientations of the fibers and tapering ratio.

Noda [15] studied temperature induced stresses in FGMs. He observed that when functionally graded materials were exposed to extreme temperature loads,

the cracks initiated in the ceramic face and propagated in the functionally graded material. The temperature stress concentration in the fgms with varying type of cracks was examined by using analytical and numerical methods. The crack propagation path due to thermal shock was studied.

Aboudi et al. [1] presented the complete generalized HSDT for FGMs based on Cartesian coordinate system. The theory was based on volumetric averaging of various quantities and bypassed the micromechanical approach based on the concept of volume element representation used in the analysis of fgm composites by specially joining the element and total responses.

Reddy [17] studied theoretical formulation and FEM model based on TSDT for FGM plate. The formulation accounted for thermo mechanical effects combining change with time and geometric nonlinearity. In this higher order theory, transverse shear stress was expressed as a quadratic function along the depth. Hence this theory requires no shear correction factor. The plate was considered as homogenous and material composition was varied along the thickness. The Young's modulus was assumed to vary as per rule of mixture in terms of the volume fractions of the material constituents.

Reddy and Cheng [18] presented thermomechanical deformation of simply supported FGM plate. The deflection along the thickness direction in the functionally graded plate was not constant when it was subjected to thermal loads. The material properties along the depth were calculated by Mori-Thanka method. The deformation due to temperature and stress of plate were calculated for the change in gradient index of ceramic material. The in plane compressive stress due to temperature load was high on the upper layer of the plate.

Biner [5] studied the thermo-elastic properties of a bi-material and an FGM by advanced finite element method. The method divides the complete model into

7

small elements using Voronoi elements. For non-homogenous sections, Voronoi element takes into account the influence of the thermal displacement. The method was checked by matching the results with the basic finite element method. The method was effective in understanding the micro-mechanical properties of FGMs.

Cho and Ha [7] presented three material property evaluation techniques. The basic rule of mixture, advanced rule of mixture and Wakashima - Tsukamoto estimating method were compared with the finite element dividing method using rectangular elements. The new rule of mixture produced a gradually varying stress change. The stress prediction by discretized model was located between linear rule and Wakashima method.

Schmauder and Weber [22] presented modeling of FGMs using numerical homogenization. The mechanical behavior of different ceramic/metal compositions was analyzed and compared with experimental studies. The microwave sintered material was possessing higher ceramic content for medium gradient index. The temperature expansion coefficient was not same as that by rule of mixture. The Young's modulus and the stress - strain behavior were simulated numerically and the influence of initial stress appeared to be less.

Shen [23] presented Nonlinear bending studies of simply supported FGM rectangular plates loaded by out of plane load and exposed to temperature environment. The constituent properties were assumed to depend on the thermal load and material properties were assumed to change along the depth as per power law. The material property was distributed according to volume components of the materials. Reddys TSDT was considered for the theoretical calculations.

Kee and Kim [11] presented the vibration analysis of a revolving composite plate. Theoretical calculation methods were obtained for pre twisted revolving shells considering the influence of centrifugal force and Coriolis acceleration.

Slightly thick cylinder shells with opening was considered with shear stress and deflection in thickness direction. FEM was used to solve the differential equation.

Huang and Shen [10] studied the dynamic reactions and free vibration including nonlinearity of FGM plate subjected to temperature. Thermal influence in the plate constituent property and heat conduction along the depth was considered. The theoretical calculations considered higher order shear deformation theory and von Karman property variation.

Dong [8] studied vibration analysis of circular plate with central hole for different edge conditions using Chebyshev Ritz method. Exponential changes in material properties along the depth of the plate was studied. Change in frequency between isotropic plate and FGM plate was studied.

Zhao et al. [31] studied free vibration analysis of bi-material FGM plate using elements free kp-Ritz method. The material properties were assumed to vary along the depth in accordance with a power-law change in material constituent fraction. FSDT was used for the formulation. In plane displacements were calculated by mesh free kernel particle function.

Bafererani et al. [3] presented an accurate solution for free vibration analysis of FGM thin circular plate with hole. The edge conditions of the plate were such that the edges were simply supported and in the inner edge the boundary condition changes. Results were given for different sector angles, inner radius to outer radius ratio and different grades of FGM.

Malekzadeh et al. [13] studied the free vibration of thick circular plate with hole exposed to temperature loads based on three dimensional elastic theory. The temperature environment effects are considered. Using Hamilton's theory, the equations of motion were obtained. The influence of material, thermal load, and

structural parameters on the fundamental frequency components were studied.

Bafererani et al [4] presented an accurate solution for free vibration problems of thin FGM plates with different edge conditions. Classical plate theory was used to create equations of motion. The Levy method was used to calculate frequencies of FGM plates for various boundary conditions.

Suresh Kumar et al. [26] presented the nonlinear bending properties and static properties of functionally graded material plate with different boundary conditions, material variation parameter, aspect ratio and length to depth ratios considering the higher order theory. The numerical results were obtained for different boundary conditions, material variation parameter, length to depth ratio, aspect ratio, and the results were validated using linear methods. The influence of nonlinearity response and deflection in the thickness direction of FGM was studied.

Singha et al. [21] presented finite element analysis of FGM plates under out of plane load considering a higher order plate bending finite element. The neutral axis position was accurately determined for the formulation. The nonlinearity of FGM plates were considered in the formulation. Transverse shear deformation factor was calculated by energy theorem.

Rath and Sahu [16] conducted numerical studies and experimental work on the free vibration characteristics of layered composite plate exposed to change in thermal load and moisture. The influence of geometry, composition of material and layer sequence of fiber composite on the free vibration with change in thermal load and moisture loads were studied.

Alibakhshi and Khavvaji [2] presented free vibration studies of simply supported thick rectangular plates modeled considering bimaterial advanced plate theory. Mass density and Young's modulus were considered according to power-

law variation. Hamilton theory was employed to derive five constitutive equations of motion. By changing geometrical parameters and boundary condition vibration analysis was carried out and influence of geometric variables on the natural frequencies were studied.

Srinivas and Shiva Prasad [25] studied the structural response of functionally graded flat thick square plate under mechanical loads. Theoretical formulation for material properties were done using the rule of mixture. Convergence studies were carried out using different mesh size and layers. Changes of displacement and stress along the depth of the plate was studied.

Wattanasakulpong [28] presented temperature dependent buckling and elastic vibration analysis of FGM beams and plates using modified TSDT. The TSDT gives a better approximation of varying material property in the thickness direction compared to FSDT. It gives a better representation of the cubic variation of displacements through the thickness over the FSDT. Critical buckling temperature results for temperature dependent material properties were solved by an iterative calculation technique. The relationship between the critical temperatures and natural frequencies of the beam and plate structures were also presented.

Thai and Choi [27] presented thickness dependent FGM Kirchhoff and Mindlin plate theory considering an improved coupled stress theory. This model contained a material variable that could represent the geometric nonlinearity, size influence and bi material variation along the depth direction. From the numerical results, it was observed that the inclusion of material variable increased the natural frequency and the deflection was reduced.

Kiani and Eslami [12] presented an exact analysis for temperature buckling of circular FGM plate with hole resting on elastic medium. The equations of equilibrium of the annular plates were derived using CPT. Temperature dependent

material properties of the plate were considered to be varying along the depth direction based on the power -law. Poissons ratio was kept constant. For different boundary problems, the buckling of supports were studied and stability equations were derived using equilibrium conditions. An accurate theoretical solution was derived to obtain the temperature buckling load by calculating eigenvalues.

Fallah et al. [9] studied analysis of medium thick rectangular FGM plates resting on flexible foundation. Free vibration analysis was considered with different combinations of simply supported and fixed boundary conditions. Mindlins plate theory was used to derive equations of motion. A semi analytical method was presented for governing equations using the extended Kantorovich method together with an infinite power series solution.

Shen et al. [24] investigated the influence of temperature and moisture conditions on the dynamic response of thick layered plates supported on a flexible foundation. The plate was modeled with the help of a micro to macro-mechanical theoretical model. The governing equations were based on HSDT and the effects of elastic foundation and moisture and temperature effects were included. The influence due to the thermal environment, foundation stiffness, moisture percentage and fiber content were presented.

2.2   Methodology

The FGM plate under consideration consists of metal on top surface and ceramic on bottom surface. The material composition changes gradually along the thickness. The rate of material property change along the thickness is indicated by a variable n (material gradient index). The plate is considered to be completely ceramic if n = 0 and the plate is completely metal if n = infinity. Material property variations are dependent on the gradient index (n) and the distance from the middle surface in the thickness direction. The material properties vary in accordance

with the power-law. (Reddy, 2000)

$$P_z = (P_t - P_b)V_f + P_b \tag{2.1}$$

$$V_f = (\frac{z}{h} + \frac{1}{2})^n \tag{2.2}$$

Where 'P' is the material property, 'z' is the distance from the center of layer under consideration to the center of plate, P_t and P_b are the property at the upper surface and lower surface respectively, V_f represents volume content of ceramic, 'n' is the gradient index. Young's modulus (E), Material density (ρ) and Poisson's ratio (ν) values change according to equation 2.1. V_f varies over the thickness as shown in Figure 2.1.
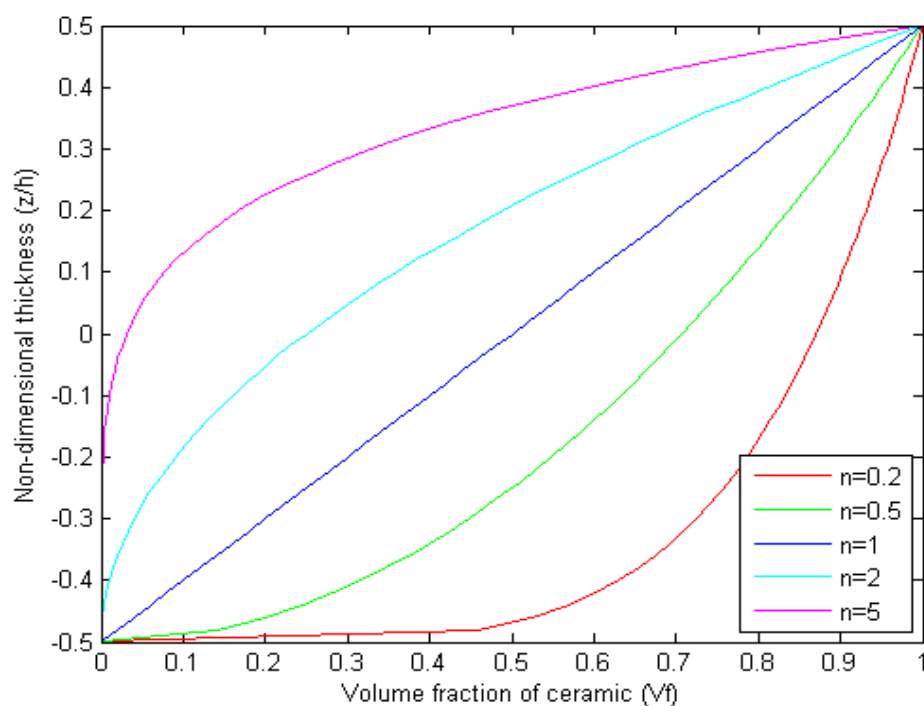
Figure 2.1: Through thickness variation of V_f

The temperature dependent material properties may be represented as a function of temperature. (Huang and Shen, 2004)

$$P = P_0(P_{-1}T^{-1} + 1 + P_1T + P_2T^2 + P_3T^3) \tag{2.3}$$

Where, $P_0, P_{-1}, P, P_1, P_2, P_3$ are temperature coefficients . These temperature coefficients are constant for each constituent material.

Modulus of elasticity (E) and coefficient of thermal expansion (α) are assumed to be dependent on temperature while thermal conductivity (κ), density (ρ) and Poisson's ratio (ν) are assumed to be constant.

$$E(z,T) = [E_t(T) - E_b(T)](\frac{z}{h} + \frac{1}{2})^n + E_b(T) \tag{2.4}$$

$$\alpha(z,T) = [\alpha_t(T) - \alpha_b(T)](\frac{z}{h} + \frac{1}{2})^n + \alpha_b(T) \tag{2.5}$$

$$\rho(z) = [\rho_t - \rho_b](\frac{z}{h} + \frac{1}{2})^n + \rho_b \tag{2.6}$$

$$\kappa(z) = [\kappa_t - \kappa_b](\frac{z}{h} + \frac{1}{2})^n + \kappa_b \tag{2.7}$$

The temperature change is considered along the depth of the plate. The temperature variation along the depth can be obtained by solving a steady state heat conduction equation. (Huang and Shen, 2004)

$$-\frac{d}{dz}\Big[\kappa(z)\frac{dT}{dz}\Big] = 0 \tag{2.8}$$

The solution of this equation is obtained by applying the boundary values of $T = T_t$ at $z = h/2$ and $T = T_b$ at $z = -h/2$. The solution can be represented as a polynomial series as (Huang and Shen. 2004)

$$T(z) = T_m + (T_c - T_m)\eta(z) \tag{2.9}$$

Where,

$$\eta(z) = \frac{1}{C}\Big[(\frac{z}{h}+\frac{1}{2}) - \frac{\kappa_{cm}}{(n+1)\kappa_m}(\frac{z}{h}+\frac{1}{2})^{(n+1)} + \frac{\kappa_{cm}{}^2}{(2n+1)\kappa_m{}^2}(\frac{z}{h}+\frac{1}{2})^{(2n+1)}$$

$$- \frac{\kappa_{cm}{}^3}{(3n+1)\kappa_m{}^3}(\frac{z}{h}+\frac{1}{2})^{(3n+1)} + \frac{\kappa_{cm}{}^4}{(4n+1)\kappa_m{}^4}(\frac{z}{h}+\frac{1}{2})^{(4n+1)}$$

$$- \frac{\kappa_{cm}{}^5}{(5n+1)\kappa_m{}^5}(\frac{z}{h}+\frac{1}{2})^{(5n+1)}\Big]$$

$$C = 1 - \frac{\kappa_{cm}}{(n+1)\kappa_m} + \frac{\kappa_{cm}{}^2}{(2n+1)\kappa_m{}^2} - \frac{\kappa_{cm}{}^3}{(3n+1)\kappa_m{}^3} + \frac{\kappa_{cm}{}^4}{(4n+1)\kappa_m{}^4} - \frac{\kappa_{cm}{}^5}{(5n+1)\kappa_m{}^5}$$

$$\kappa_{cm} = \kappa_c - \kappa_m$$

As the material properties of the FGM changes along the depth, the numerical model is divided in to a number of layers such that it gives the change in properties. Each layer is considered to be isotropic. To calculate the material property in each layer powerlaw (Eq 2.1) variation is assumed . The laminated structure represents the step wise change in properties, by using a high number of layers the gradation can be approximated.
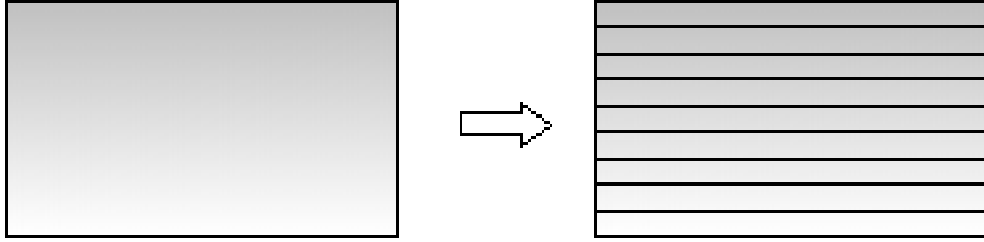
Figure 2.2: FGM section and equivalent laminated composite section

A MATLAB code based on finite element method is prepared for the computation. The MATLAB code is checked by comparing the results of flat FGM plates with published results. Shell element is used to model the thin twisted plate. Convergence studies are done to find out the suitable mesh size and number of layers to get accurate results.

2.3   Objective of the present study

Literature review shows there are a lot of studies in the field of free vibration analysis of flat FGM plate. In the field of twisted FGM plate, very little research work have been done. This thesis deals with the vibration analysis of cantilever twisted FGM plates. The study aims to model the twisted plate using shell element, and solve the free vibration problem using finite element method. The influence of various factors such as thermal environment and geometrical variables on the natural frequencies are studied.

Chapter 3

FORMULATION

Chapter 3

FORMULATION

3.1 Twisted plate characteristics
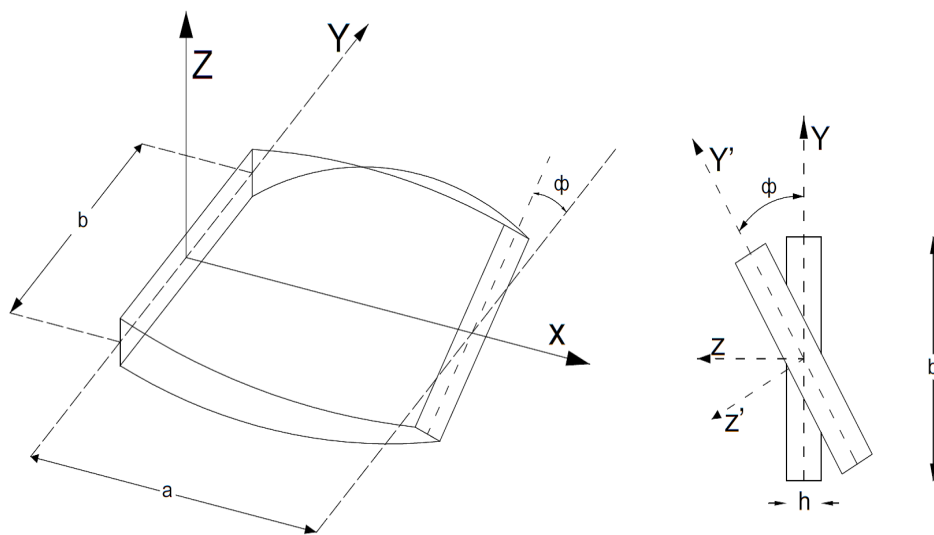
Figure 3.1: Laminated twisted plate

The Figure 3.1 shows a Twisted FGM plate.

Here,

ϕ= angle of twist.

a and b are length and width of the plate respectively.

h is the thickness of plate.

3.2 Governing differential equations

Consider a small pretwisted element with radius of curvature R_x and R_y in x and y directions. The forces acting on the twisted plate element are $(N_x, N_y, \text{and } N_{xy})$ in plane forces, shearing forces $(Q_x, \text{and } Q_y)$ and the bending moment components $(M_x, M_y \text{ and } M_{xy})$. The differential equations of equilibrium for pretwisted doubly curved shell panel is given as (Sahu and Datta [20] , Chandrashekhara [6]):

$$\frac{\partial N_x}{\partial x} + \frac{\partial N_{xy}}{\partial y} - \frac{1}{2}\left(\frac{1}{R_y} - \frac{1}{R_x}\right)\frac{\partial M_{xy}}{\partial y} + \frac{Q_x}{R_x} + \frac{Q_y}{R_{xy}} = P_1\frac{\partial^2 u}{\partial t^2} + P_2\frac{\partial^2 \theta_x}{\partial t^2}$$

$$\frac{\partial N_{xy}}{\partial x} + \frac{\partial N_y}{\partial y} + \frac{1}{2}\left(\frac{1}{R_y} - \frac{1}{R_x}\right)\frac{\partial M_{xy}}{\partial x} + \frac{Q_y}{R_y} + \frac{Q_x}{R_{xy}} = P_1\frac{\partial^2 v}{\partial t^2} + P_2\frac{\partial^2 \theta_y}{\partial t^2}$$

$$\frac{\partial Q_x}{\partial x} + \frac{\partial Q_y}{\partial y} - \frac{N_x}{R_x} - \frac{N_y}{R_y} - 2\frac{N_{xy}}{R_{xy}} + N_x{}^0\frac{\partial^2 w}{\partial x^2} + N_y{}^0\frac{\partial^2 w}{\partial y^2} = P_1\frac{\partial^2 w}{\partial t^2} \qquad (3.1)$$

$$\frac{\partial M_x}{\partial x} + \frac{\partial M_{xy}}{\partial y} - Q_x = P_3\frac{\partial^2 \theta x}{\partial t^2} + P_2\frac{\partial^2 u}{\partial t^2}$$

$$\frac{\partial M_{xy}}{\partial x} + \frac{\partial M_y}{\partial y} - Q_y = P_3\frac{\partial^2 \theta y}{\partial t^2} + P_2\frac{\partial^2 v}{\partial t^2}$$

Where,

$N_x{}^0$ and $N_y{}^0$ are external in plane force in 'x' and 'y' direction respectively.

R_x and R_y are the radii of curvature in the 'x' and 'y' directions respectively.

R_{xy} is the radius of twist.

$$(P_1, P_2, P_3) = \sum_{k=1}^{n}\int_{z_{k-1}}^{z_k}(\rho)_k(1, z, z^2)\partial z \qquad (3.2)$$

Where,

n = number of layers considered.

ρ_k =Density at kth layer .

3.3 Free vibration analysis

The governing equation for free vibration analysis is given by:

$$[M]\{\ddot{q}\} + [K]\{q\} = 0 \qquad (3.3)$$

$$[K] - \omega_n{}^2[M] = 0 \qquad (3.4)$$

Where, [M] is the mass matrix, ω_n is the natural frequencies, [K] is the stiffness matrix, and $\{q\}$ is the vector of degrees of freedom.

Considering a plate subjected to thermal environment the governing equation becomes,

$$[M]\{\ddot{q}\} + ([K] + [K_g])\{q\} = 0 \qquad (3.5)$$

$$[K] + [K_g] - \omega_n{}^2[M] = 0 \qquad (3.6)$$

Where,

$[K_g]$ is the initial stress stiffness matrix due to temperature stress.

3.3.1 Constitutive relations

The constitutive relations for the composite plate exposed to thermal load is given by.

$$\{F\} = [D]\{\epsilon\} - \{F^N\} \qquad (3.7)$$

Where,

$$\{F\} = \{N_x \ N_y \ N_{xy} \ M_x \ M_y \ M_{xy} \ Q_x \ Q_y\}^T \qquad (3.8)$$

$$\{F^N\} = \{N_x{}^N \ N_y{}^N \ N_{xy}{}^N \ M_x{}^N \ M_y{}^N \ M_{xy}{}^N \ 0 \ 0\}^T \qquad (3.9)$$

$$\{\epsilon\} = \{\epsilon_x \ \epsilon_y \ \epsilon_{xy} \ K_x \ K_y \ K_{xy} \ \phi_x \ \phi_y\}^T \qquad (3.10)$$

$$D = \begin{bmatrix} A_{11} & A_{12} & A_{16} & B_{11} & B_{12} & B_{16} & 0 & 0 \\ A_{21} & A_{22} & A_{26} & B_{21} & B_{22} & B_{26} & 0 & 0 \\ A_{61} & A_{62} & A_{66} & B_{61} & B_{62} & B_{66} & 0 & 0 \\ B_{11} & B_{12} & B_{16} & D_{11} & D_{12} & D_{16} & 0 & 0 \\ B_{21} & B_{22} & B_{26} & D_{21} & D_{22} & D_{26} & 0 & 0 \\ B_{61} & B_{62} & B_{66} & D_{61} & D_{62} & D_{66} & 0 & 0 \\ 0 & 0 & 0 & 0 & 0 & 0 & S_{44} & S_{45} \\ 0 & 0 & 0 & 0 & 0 & 0 & S_{54} & S_{55} \end{bmatrix} \qquad (3.11)$$

In plane forces and bending moment resultants due to thermal load can be represented as:

$$\{N_x{}^N \ N_y{}^N \ N_{xy}{}^N\}^T = \sum_{k=1}^{n} (Q_{ij})_k \{\epsilon_k\}(z_k - z_{k-1}) \quad \text{For i,j=1,2,6} \quad (3.12)$$

$$\{M_x{}^N \ M_y{}^N \ M_{xy}{}^N\}^T = \frac{1}{2}\sum_{k=1}^{n} (Q_{ij})_k \{\epsilon_k\}(z_k{}^2 - z_{k-1}{}^2) \quad \text{For i,j=1,2,6} \quad (3.13)$$

$$\{\epsilon\}_N = \{\epsilon_{xN} \ \epsilon_{yN} \ \epsilon_{xyN}\}^T = \{\alpha \ \alpha \ 0\}^T (T - T_0) \quad (3.14)$$

Coefficients of stiffness are defined as:

$$(A_{ij}, B_{ij}, D_{ij}) = \sum_{k=1}^{n} \int_{z_{k-1}}^{z_k} [Q_{ij}]_k (1, z, z^2)\partial z \quad \text{for i,j=1,2,6} \quad (3.15)$$

$$S_{ij} = \frac{5}{6}\sum_{k=1}^{n} \int_{z_{k-1}}^{z_k} [Q_{ij}]_k \partial z. \quad (3.16)$$

A coefficient of $\frac{5}{6}$ is considered in S_{ij} calculations as a shear correction factor .

$$[Q] = \begin{bmatrix} Q_{11} & Q_{12} & 0 & 0 & 0 \\ Q_{21} & Q_{22} & 0 & 0 & 0 \\ 0 & 0 & Q_{66} & 0 & 0 \\ 0 & 0 & 0 & Q_{44} & 0 \\ 0 & 0 & 0 & 0 & Q_{55} \end{bmatrix} \quad (3.17)$$

$$Q_{11} = Q_{22} = \frac{E}{(1 - \nu^2)}$$

$$Q_{12} = Q_{21} = \frac{\nu E}{(1 - \nu^2)}$$

$$Q_{44} = Q_{55} = Q_{66} = \frac{E}{2(1 + \nu)}$$

21

3.3.2 Strain Displacement Relations

Green-Lagranges strain displacement relations are used in this analysis. The total strain is divided in to linear strain and non linear strain. The linear strain considered to derive the stiffness matrix. The non linear strain part is considered in the derivation of initial stress stiffness matrix.

$$\{\epsilon\} = \{\epsilon_l\} + \{\epsilon_{nl}\} \tag{3.18}$$

The linear strain components for a twisted shell element is given by:

$$
\begin{aligned}
\epsilon_{xl} &= \frac{\partial u}{\partial x} + \frac{w}{R_x} + zk_x \\
\epsilon_{yl} &= \frac{\partial v}{\partial y} + \frac{w}{R_y} + zk_y \\
\Upsilon_{xyl} &= \frac{\partial u}{\partial y} + \frac{\partial v}{\partial x} + \frac{2w}{R_{xy}} + zk_{xy} \\
\Upsilon_{xzl} &= \frac{\partial w}{\partial x} + \theta_x - \frac{u}{R_x} - \frac{v}{R_{xy}} \\
\Upsilon_{yzl} &= \frac{\partial w}{\partial y} + \theta_y - \frac{v}{R_y} - \frac{u}{R_{xy}}
\end{aligned}
\tag{3.19}
$$

The bending strain components are given by.

$$
\begin{aligned}
k_x &= \frac{\partial \theta_x}{\partial x} \\
k_y &= \frac{\partial \theta_y}{\partial y} \\
k_{xy} &= \frac{\partial \theta_x}{\partial y} + \frac{\partial \theta_y}{\partial x} + \frac{1}{2}(\frac{1}{R_y} - \frac{1}{R_x})(\frac{\partial v}{\partial x} - \frac{\partial u}{\partial y})
\end{aligned}
\tag{3.20}
$$

The nonlinear strain components are given by

$$
\begin{aligned}
\epsilon_{xnl} &= \frac{1}{2}(\frac{\partial u}{\partial x})^2 + \frac{1}{2}(\frac{\partial v}{\partial x})^2 - \frac{1}{2}(\frac{\partial w}{\partial x} - \frac{u}{R_x})^2 + \frac{1}{2}z^2\Big[(\frac{\partial \theta_x}{\partial x})^2 + (\frac{\partial \theta_y}{\partial x})^2\Big] \\
\epsilon_{ynl} &= \frac{1}{2}(\frac{\partial u}{\partial y})^2 + \frac{1}{2}(\frac{\partial v}{\partial y})^2 - \frac{1}{2}(\frac{\partial w}{\partial y} - \frac{u}{R_y})^2 + \frac{1}{2}z^2\Big[(\frac{\partial \theta_x}{\partial y})^2 + (\frac{\partial \theta_y}{\partial y})^2\Big] \\
\Upsilon_{xynl} &= \frac{\partial u}{\partial x}(\frac{\partial u}{\partial y}) + \frac{\partial v}{\partial x}(\frac{\partial v}{\partial y}) + (\frac{\partial w}{\partial x} - \frac{u}{Rx})(\frac{\partial w}{\partial y} - \frac{v}{Ry}) \\
&\quad + z^2\Big[(\frac{\partial \theta_x}{\partial x})(\frac{\partial \theta_x}{\partial y}) + (\frac{\partial \theta_y}{\partial x})(\frac{\partial \theta_y}{\partial y})\Big]
\end{aligned}
\tag{3.21}
$$

3.4 Finite element formulation

Finite element method can be used for complex shape and boundary conditions were analytical methods are not so easily applicable. Using the First order shear deformation theory the finite element formulation was developed for the structural analysis of FGM pretwisted shell elements. The plate is assumed to be consisting of a number layers, where each layer is considered to be homogenous and isotropic. An eight noded isoparametric quadratic shell element is used in analysis. The shell element consists of midsurface nodes. Each node has five degrees of freedom u,v,w,θ_x and θ_y. The Jacobian matrix transfers the isoparametric element in natural coordinate system into Cartesian coordinate system. The Figure 3.2 shows 8 noded isoparametric element with node numbers. The shape function for 8 noded shell element is given by,

$$u(\xi, \eta) = \alpha_1 + \alpha_2\xi + \alpha_3\eta + \alpha_4\xi^2 + \alpha_5\xi\eta + \alpha_6\eta^2 + \alpha_7\xi^2\eta + \alpha_8\xi\eta^2 \qquad (3.22)$$

The shape function represent the displacement between nodes N_i.

$$
\begin{aligned}
N_i &= (1 + \xi\xi_i)(1 + \eta\eta_i)\frac{(\xi\xi_i + \eta\eta_i - 1)}{4} && \text{i=1 to 4} \\
N_i &= (1 - \xi^2)\frac{1 + \eta\eta_i}{2} && \text{i=5,7} \\
N_i &= (1 + \xi\xi_i)\frac{(1 - \eta^2)}{2} && \text{i=6,8}
\end{aligned}
\qquad (3.23)
$$

Where ξ and η are the natural coordinates of the element and ξ_i and η_i are the values at i th node. The derivatives of the shape function (N_i) with respect to Cartesian coordinate 'x' and 'y' can be converted to natural coordinate (ξ and η) by

$$\begin{bmatrix} N_{i,x} \\ N_{i,y} \end{bmatrix} = [J]^{-1} \begin{bmatrix} N_{i,\xi} \\ N_{i,\eta} \end{bmatrix} \qquad (3.24)$$

$$[J] = \begin{bmatrix} X_{i,\xi} & Y_{i,\xi} \\ X_{i,\eta} & Y_{i,\eta} \end{bmatrix} \qquad (3.25)$$
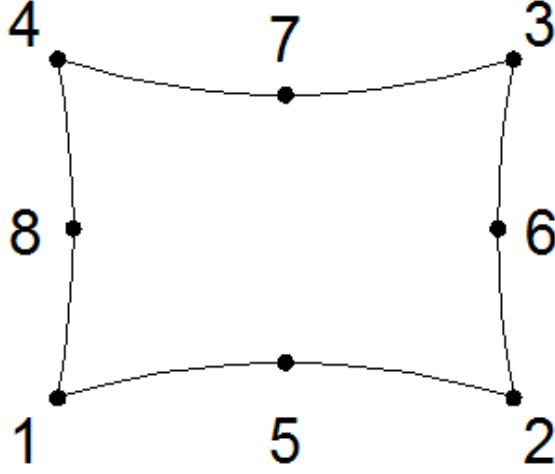
Figure 3.2: Isoparametric quadratic shell element

Where, [J] is the Jacobian matrix.

Based on the FSDT the displacement field is given by

$$u(x, y, z) = u_0(x, y) + z\theta_x(x, y)$$

$$v(x, y, z) = v_0(x, y) + z\theta_y(x, y) \tag{3.26}$$

$$w(x, y, z) = w_0(x, y)$$

Where, u, v and w are displacement in the x, y and z directions respectively

u_0, v_0, w_0 are displacement at the midplane in the x, y and z directions respectively

θ_x and θ_y are the rotations of the midplane normal to the x and y axes respectively.

The displacements calculated from shape function as

$$x = \sum N_i x_i, \quad y = \sum N_i y_i$$

$$u_0 = \sum N_i u_i, \quad v_0 = \sum N_i v_i \quad w_0 = \sum N_i w_i \tag{3.27}$$

$$\theta_x = \sum N_i \theta_{xi}, \quad \theta_y = \sum N_i \theta_{yi}$$

24

3.4.1 Derivation of element elastic stiffness matrix

The linear strain components can be expresses in term of displacements as:

$$\{\epsilon\} = [B]\{d_e\} \tag{3.28}$$

Where,

$$\{d_e\} = \{u_1 \ v_1 \ w_1 \ \theta_{x1} \ \theta_{y1} \ \ldots \ u_8 \ v_8 \ w_8 \ \theta_{x8} \ \theta_{y8}\} \tag{3.29}$$

$$[B] = [[B_1] \ [B_2] \ \ldots \ [B_8]] \tag{3.30}$$

$$[B_i] = \begin{bmatrix} N_{i,x} & 0 & \frac{N_i}{R_x} & 0 & 0 \\ 0 & N_{i,y} & \frac{N_i}{R_y} & 0 & 0 \\ N_{i,y} & N_{i,x} & \frac{2N_i}{R_{xy}} & 0 & 0 \\ 0 & 0 & 0 & N_{i,x} & 0 \\ 0 & 0 & 0 & 0 & N_{i,y} \\ 0 & 0 & 0 & N_{i,y} & Ni,x \\ \frac{-N_i}{R_x} & \frac{-N_i}{R_{xy}} & N_{i,x} & N_i & 0 \\ \frac{-N_i}{R_{xy}} & \frac{-N_i}{R_y} & N_{i,y} & 0 & N_i \end{bmatrix} \tag{3.31}$$

Element elastic stiffness matrix is given by

$$[ke] = \int_{-1}^{1} \int_{-1}^{1} [B]^T [D][B]|J|d\xi d\eta \tag{3.32}$$

3.4.2 Derivation of element initial stress stiffness matrix

The non-linear strain components can be expressed in matrix form:

$$\epsilon_{nl} = \{\epsilon_{xnl} \ \epsilon_{ynl} \ \gamma_{xynl}\}^T = \frac{[R]\{d\}}{2} \tag{3.33}$$

Where,

$$\{d\} = \{u_x \ u_y \ v_x \ v_y \ w_x \ w_y \ \theta_{x,x} \ \theta_{x,y} \ \theta_{y,x} \ \theta_{y,y} \ \theta_x \ \theta_y\}^T \tag{3.34}$$

Displacement $\{d\}$ can be expressed as

$$\{d\} = [G]\{d_e\} \tag{3.35}$$

$$[G] = \sum_{i=1}^{8} \begin{bmatrix} N_{i,x} & 0 & 0 & 0 & 0 \\ N_{i,y} & 0 & 0 & 0 & 0 \\ 0 & N_{i,x} & 0 & 0 & 0 \\ 0 & N_{i,y} & 0 & 0 & 0 \\ 0 & 0 & N_{i,x} & 0 & 0 \\ 0 & 0 & N_{i,y} & 0 & 0 \\ 0 & 0 & 0 & N_{i,x} & 0 \\ 0 & 0 & 0 & N_{i,y} & 0 \\ 0 & 0 & 0 & 0 & N_{i,x} \\ 0 & 0 & 0 & 0 & N_{i,y} \end{bmatrix} \tag{3.36}$$

The element initial stress stiffness matrix due to thermal stress is given by:

$$[k_g]_e = \int_{-1}^{1} \int_{-1}^{1} [G]^T [S] [G] |J| d\xi d\eta \tag{3.37}$$

Where,

$$[S] = \begin{bmatrix} S_{11} & S_{21} & 0 & 0 & 0 & 0 & 0 & 0 & S_{91} & S_{101} & 0 & S_{121} \\ S_{21} & S_{22} & 0 & 0 & 0 & 0 & 0 & 0 & S_{92} & S_{102} & 0 & S_{122} \\ 0 & 0 & S_{33} & S_{43} & 0 & 0 & S_{73} & S_{83} & 0 & 0 & S_{113} & 0 \\ 0 & 0 & S_{43} & S_{44} & 0 & 0 & S_{74} & S_{84} & 0 & 0 & S_{114} & 0 \\ 0 & 0 & 0 & 0 & S_{55} & S_{65} & 0 & 0 & 0 & 0 & 0 & 0 \\ 0 & 0 & 0 & 0 & S_{65} & S_{66} & 0 & 0 & 0 & 0 & 0 & 0 \\ 0 & 0 & S_{73} & S_{74} & 0 & 0 & S_{77} & S_{87} & 0 & 0 & 0 & 0 \\ 0 & 0 & S_{83} & S_{84} & 0 & 0 & S_{87} & S_{88} & 0 & 0 & 0 & 0 \\ S_{91} & S_{92} & 0 & 0 & 0 & 0 & 0 & 0 & S_{99} & S_{109} & 0 & 0 \\ S_{101} & S_{102} & 0 & 0 & 0 & 0 & 0 & 0 & S_{109} & S_{1010} & 0 & 0 \\ 0 & 0 & S_{113} & S_{114} & 0 & 0 & 0 & 0 & 0 & 0 & 0 & 0 \\ S_{113} & S_{114} & 0 & 0 & 0 & 0 & 0 & 0 & 0 & 0 & 0 & 0 \end{bmatrix} \tag{3.38}$$

26

$$S_{11} = S_{33} = S_{55} = N_x{}^r, \qquad\qquad S_{22} = S_{44} = S_{66} = N_y{}^r$$

$$S_{21} = S_{43} = S_{65} = N_{xy}{}^r, \qquad\qquad S_{77} = S_{99} = \frac{N_x{}^r t^2}{12}$$

$$S_{88} = S_{1010} = \frac{N_y{}^r t^2}{12}, \qquad\qquad S_{87} = S_{109} = \frac{N_{xy}{}^r t^2}{12}$$

$$-S_{73} = S_{91} = M_x{}^r, \qquad\qquad -S_{84} = S_{102} = M_y{}^r$$

$$-S_{113} = S_{121} = Q_x{}^r, \qquad\qquad -S_{114} = S_{122} = Q_y{}^r$$

$$-S_{74} = -S_{83} = S_{92} = S_{101} = M_{xy}{}^r$$

3.4.3   Derivation of element mass matrix

The element mass matrix is given by

$$[m_e] = \int_{-1}^{1} \int_{-1}^{1} [N]^T [P][N] |J| d\xi d\eta \tag{3.39}$$

Where the shape function matrix

$$[N] = \begin{bmatrix} N_i & 0 & 0 & 0 & 0 \\ 0 & N_i & 0 & 0 & 0 \\ 0 & 0 & N_i & 0 & 0 \\ 0 & 0 & 0 & N_i & 0 \\ 0 & 0 & 0 & 0 & N_i \end{bmatrix} \quad for\ i = 1, 2, \ldots 8 \tag{3.40}$$

$$[P] = \begin{bmatrix} P_1 & 0 & 0 & P_2 & 0 \\ 0 & P_1 & 0 & 0 & P_2 \\ 0 & 0 & P_1 & 0 & 0 \\ P_2 & 0 & 0 & P_3 & 0 \\ 0 & P_2 & 0 & 0 & P_3 \end{bmatrix} \tag{3.41}$$

$$(P_1, P_2, P_3) = \sum_{k=1}^{n} \int_{z_{k-1}}^{z_k} (\rho)_k (1, z, z^2) dz \tag{3.42}$$

Where [B] - is the strain-displacement matrix, [D] - is the stress-strain matrix, [N]- is the shape function matrix $|J|$ is the determinant of Jacobian matrix. [P]- is the mass density parameters.

Chapter 4

RESULTS AND DISCUSSIONS

Chapter 4

Results and Discussions

4.1 Introduction

In this chapter, the results of the free vibration analysis of FGM twisted cantilever panels are presented. A MATLAB code based on FEM is written for the computations. The 8 noded isoparametric shell element is used for the analysis. The mesh size and number of layers required to get accurate results are fixed by conducting the convergence study. The results are compared with previous studies in order to validate the modelling using MATLAB code.

4.2 Convergence study

The convergence study is conducted for the mesh size or number of divisions required for the finite element analysis. Second convergence study is conducted for the number of layers required to represent the FGM. First three lowest non dimensional frequencies of free vibration of the FGM square plate are considered and the results are compared with previous studies. For this study an Al/Al_2O_3 FGM square flat plate with a/b =1, b/h=100, (where a, b, h are width, length and thickness of the plate respectively) was taken. The material properties are Al - (Density = $2707kg/m^3$, Young's modulus = 70GPa, Poisson's ratio = 0.3), Al/Al_2O_3 - (Density =$3800kg/m^3$, Young's modulus =380GPa, Poisson's ratio=0.3). Boundary condition - all sides are simply supported.

Non-dimensional frequency ($\omega*$) is given by

$$\omega* = \frac{\omega \pi^2 a^2}{t} \sqrt{\frac{\rho_m}{E_m}} \tag{4.1}$$

Convergence study for number of mesh divisions is done first. The convergence studies are conducted on a simply supported isotropic plate (n=0). The first four frequencies are observed with increase in number of mesh divisions. The Table 4.1 shows the observations. The results show good convergence for mesh division 10×10. The mesh division 10×10 is used for further study.

Table 4.1: Convergence of Non-dimensional frequency ($\omega*$) with varying mesh size $n = 0$

Mesh division	Non-dimensional frequency ($\omega*$)		
	1st frequency	$2^{nd} and$ 3rd frequency	4th frequency
4 x 4	116.80	306.25	631.86
6 x 6	115.94	290.80	473.02
8 x 8	115.90	289.86	464.33
10 x 10	115.90	289.68	463.39
12 x 12	115.89	289.62	463.19
Ref [30]	115.89	289.58	463.07

The FGM section is considered as an equivalent laminate section for the finite element modeling. Convergence study is conducted for determining the number of layers required to represent the FGM property accurately. The convergence study is done by using Al/Al_2O_3 simply supported FGM plate with gradient index=1. The first four non-dimensional frequencies are observed with increase in number of layers. The observations are given in Table 4.2. From the observations, it is concluded that 50 number of layers is sufficient to represent the FGM property as an equivalent laminated section. The further analysis is conducted using 50 numbers of layers.

Table 4.2: Convergence of Non-dimensional frequency ($\omega*$) with number of layers ($n = 1$)

Mesh division	Non-dimensional frequency ($\omega*$)		
	1st frequency	$2^{nd} and\ 3^{rd}$ frequency	4th frequency
4	89.24	223.58	357.17
6	88.70	222.22	355.01
12	88.42	221.51	353.87
36	88.44	221.08	353.69
50	88.44	221.06	353.66
80	88.43	221.05	353.65
Ref [30]	88.43	220.97	353.38

4.3   Comparison with previous studies

The FGM plate modeling as an equivalent laminated section and the finite element formulation using MATLAB code is validated by comparing the non-dimensional frequencies with published results. First the FGM section is validated by comparing the non-dimensional frequencies of simply supported square FGM plate. Table 4.3 gives the comparison of Non-dimensional fundamental frequencies with published results, by changing the material property index for Al/Al_2O_3 (a/b=1, b/h=100). All edges of the plate are taken as simply supported. From Table 4.3 it is observed that the non-dimensional frequencies obtained by the present formulation for the different gradient index are almost same. First four modes of vibrations are compared in this table.

To validate the twisted plate modeling, the free vibration results of isotropic twisted plate results are compared. For different angle of twist non dimensional frequencies of vibration are checked. Four modes of vibration considered in the study are first bending mode (1B), Second bending mode (2B), Twisting mode (1T), Chord wise bending mode (CB). The four mode shapes are plotted using MATLAB code. The different mode shape profiles are shown in Figure 4.1. The

Table 4.3: Non-dimensional frequency ($\omega*$) of Al/Al_2O_3 with varying material property index (a/b=1, b/h=100, $\phi = 0$)

Gradient index	Mode 1		Mode 2 & 3		Mode 3	
	Present study	FSDT Ref [30]	Present study	FSDT Ref [30]	Present study	FSDT Ref [30]
n=0	115.90	115.89	289.68	289.58	463.39	463.07
n=0.5	98.16	98.13	245.36	245.22	392.51	392.15
n=1	88.43	88.42	221.05	220.97	353.64	353.38
n=2	80.40	80.39	200.96	200.89	321.49	321.27

three dimensional mode shapes are shown in Figure 4.2. The comparison of non-dimensional frequencies (λ) of cantilever isotropic plate for different angle of twist with published results Ref [11], Ref [14] are shown in Table 4.4. The plate dimensions are (a/b =1, b/h = 20, E = 200GPa, $\nu = 0.3$).

Non-dimensional frequency (λ) is given by

$$\lambda = \omega a^2 \sqrt{\frac{\rho h}{D}} \qquad (4.2)$$

Where,

$$D = \frac{Eh^3}{12(1-\nu^2)}$$

Table 4.4: Non-dimensional frequency (λ) of cantilever twisted isotropic plate

Angle of Twist	Mode	Ref [14]	Ref [11]	Present study
0	1B	3.46	3.49	3.46
	2B	21.44	22.01	20.89
	1T	8.53	8.51	8.33
	1CB	27.05	27.33	26.64
30	1B	3.41	3.42	3.40
	2B	18.88	19.51	18.79
	1T	16.88	14.43	15.95
	1CB	27.98	27.41	27.33
45	1B	3.36	3.35	3.32
	2B	16.51	17.22	16.26
	1T	22.31	20.45	24.33
	1CB	30.40	28.76	29.89

The temperature depended material properties, temperature variation along the thickness direction and the influence of temperature initial stress are validated by comparing free vibration analysis in thermal environment. Simply supported FGM square plate made up of $Si_3N_4/SUS304$ is considered in the study. For different ceramic temperature and different gradient index, the free vibration frequencies are observed and the results are compared with the published results, the observations are given in Table 4.7. The plate dimensions considered in the study are a/h=8, a/b=1. The temperature dependent coefficients for calculating material property at different temperature is given in Table 4.5. The material properties are given in Table 4.6.

The natural frequency parameter (Ω)

$$\Omega = \frac{\omega a^2}{h} \left[\frac{\rho_m(1-\nu^2)}{E_{m_0}} \right]^{\frac{1}{2}} \tag{4.3}$$

33

(a) 1st bending mode

(b) 2nd bending mode

(c) 1st twisting mode

(d) 1st chordwise bending
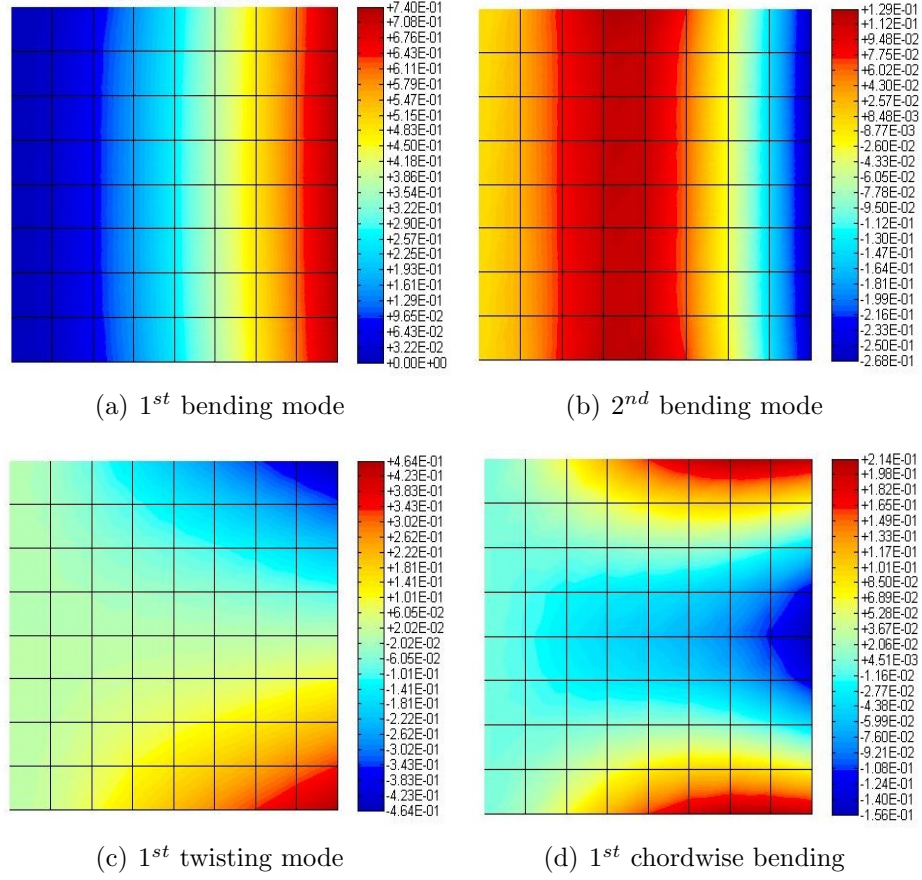
Figure 4.1: First four mode shape profile of 45^0 twisted cantilever plate

Table 4.5: Temperature dependent coefficients (Huang and Shen,2004)

Material	Properties	P_0	P_{-1}	P_1	P_2	P_3
Si_3N_4	E(Pa)	348.43×10^9	0	-3.07×10^{-4}	2.160×10^{-7}	-8.946×10^{-11}
	$\alpha(1/K)$	5.8723×10^{-6}	0	9.095×10^{-4}	0	0
SUS304	E(Pa)	201.04×10^9	0	3.079×10^{-4}	-6.534×10^{-7}	0
	$\alpha(1/K)$	12.330×10^{-6}	0	$8.086 \times 10^{-}4$	0	0
ZrO_2	E(Pa)	244.27×10^9	0	-1.371×10^{-3}	1.214×10^{-6}	-3.681×10^{-10}
	$\alpha(1/K)$	12.766×10^{-6}	0	-1.491×10^{-3}	1.006×10^{-5}	-6.778×10^{-11}
Ti-6Al-4V	E(Pa)	122.56×10^9	0	-4.586×10^{-4}	0	0
	$\alpha(1/K)$	7.5788×10^{-6}	0	6.638×10^{-4}	-3.147×10^{-6}	0

34

(a) 1st bending mode

(b) 2nd bending mode

(c) 1st twisting mode

(d) 1st chordwise bending

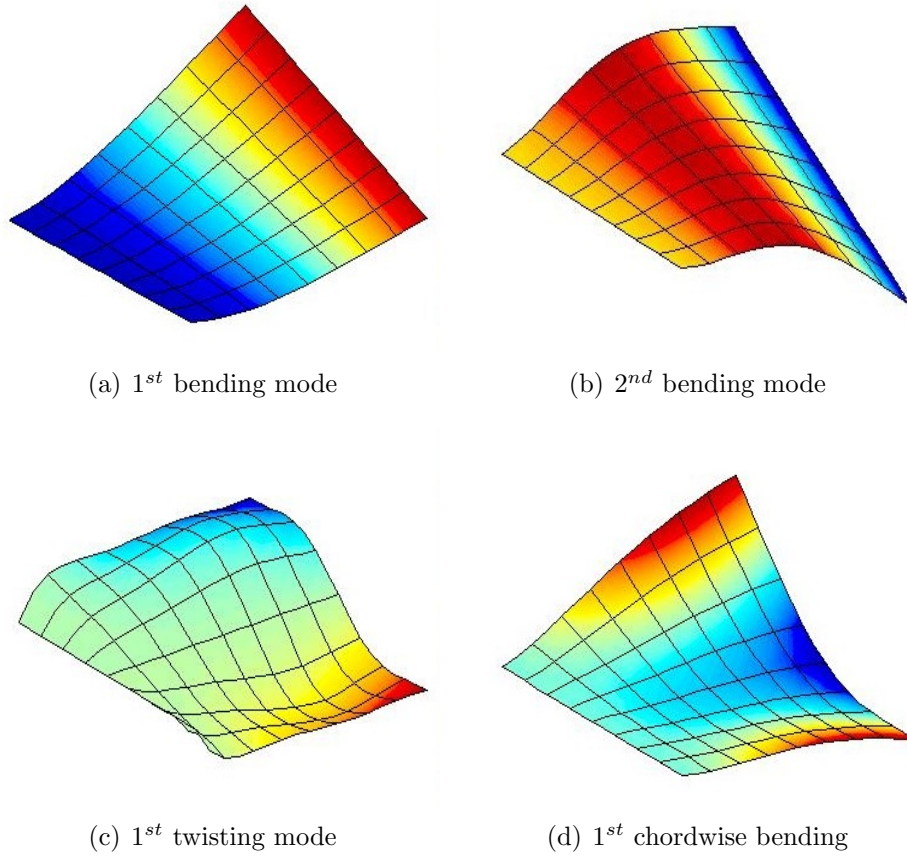Figure 4.2: First four mode shape of 45^0 twisted cantilever plate

Table 4.6: Material properties (Huang and Shen, 2004)

Material	Density $(kg/m^3$	Thermal Conductivity (κ) (W/mK)	Poisson's ratio
Si_3N_4	2370	9.19	0.28
SUS304	8166	12.04	0.28
ZrO_2	3000	1.80	0.3
Ti-6Al-4V	4429	7.82	0.3

Table 4.7: Comparison of natural frequency parameter for $Si_3N_4/SUS304$ in thermal environment (a/h=8,a/b=1)

Temperature	Gradient index (n)	Mode 1		Mode 2		Mode 3	
		Present study	Ref [27]	Present study	Ref [27]	Present study	Ref [27]
Tc=300K Tm=300K	0	12.501	12.495	29.272	29.131	44.245	43.845
	0.5	8.609	8.675	20.142	20.262	30.441	30.359
	1	7.545	7.555	17.649	17.649	26.668	26.606
	2	6.775	6.777	15.839	15.809	23.923	23.806
Tc=400K Tm=300K	0	12.308	12.397	28.976	29.083	48.863	43.835
	0.5	8.453	8.615	19.925	20.215	30.168	30.530
	1	7.398	7.474	17.451	17.607	26.423	26.590
	2	6.635	6.693	15.654	15.762	23.697	23.786
Tc=600K Tm=300K	0	11.888	11.984	28.385	28.504	43.115	43.107
	0.5	8.118	8.269	19.476	19.783	29.615	29.998
	1	7.082	7.171	17.033	17.213	25.914	26.104
	2	6.326	6.398	15.253	15.384	23.210	23.237

4.4   Free vibration analysis

Free vibration analysis of cantilever twisted Al/Al_2O_3 FGM plate is studied. The plate characteristics are a/b =1, b/h=100. The material properties are

Al - (Density = 2707 kg/m^3, Youngs modulus = 70GPa, Poissons ratio = 0.3),

Al_2O_3 - (Density=3800 kg/m^3, Young's modulus =380GPa, Poisson's ratio=0.3)

The influence of aspect ratio on the free vibration of pretwisted plate is studied first. For this study an Al/Al_2O_3 twisted FGM plate with gradient index n =1 and angle of twist $\phi = 15^0$ is taken. Other dimensions are a=1, a/h=100. First four natural frequencies are observed for different aspect ratio. Table 4.8 shows the observations. With the increase in aspect ratio the frequencies are observed to be decreasing. Figure 4.3 shows this variation for fundamental frequency.

Table 4.8: Natural frequencies (ω) in Hz of cantilever Twisted Al/Al_2O_3 FGM plate with varying a/b ratio. (n=1,a=1m,a/h=100,$\phi = 15^0$)

a/b ratio	1st frequency	2nd frequency	3rd frequency	4th frequency
1	12.724	77.108	119.82	135.140
1.5	5.644	34.178	82.052	94.286
2	3.165	19.175	37.027	54.792
2.5	2.019	12.246	24.705	35.028
3	1.399	8.489	17.830	24.277

The effect of angle of twist is studied secondly. Cantilever twisted Al/Al_2O_3 FGM plate is considered in the study with gradient index=1 and other plate dimensions are a/b=1 and a/h=100. The angle of twist changes from 0^0 to 45^0. The change in first four non-dimensional frequencies are observed. Table 4.9 gives the results of the vibration study. The fundamental frequencies decrease slightly with an increase in angle of twist.

The influence of gradient index on the free vibration of pretwisted Al/Al_2O_3 FGM plate is studied. The FGM plate with angle of twist 20^0 and a/b =1, a/h=100 are taken for the analysis. The change in non-dimensional frequencies
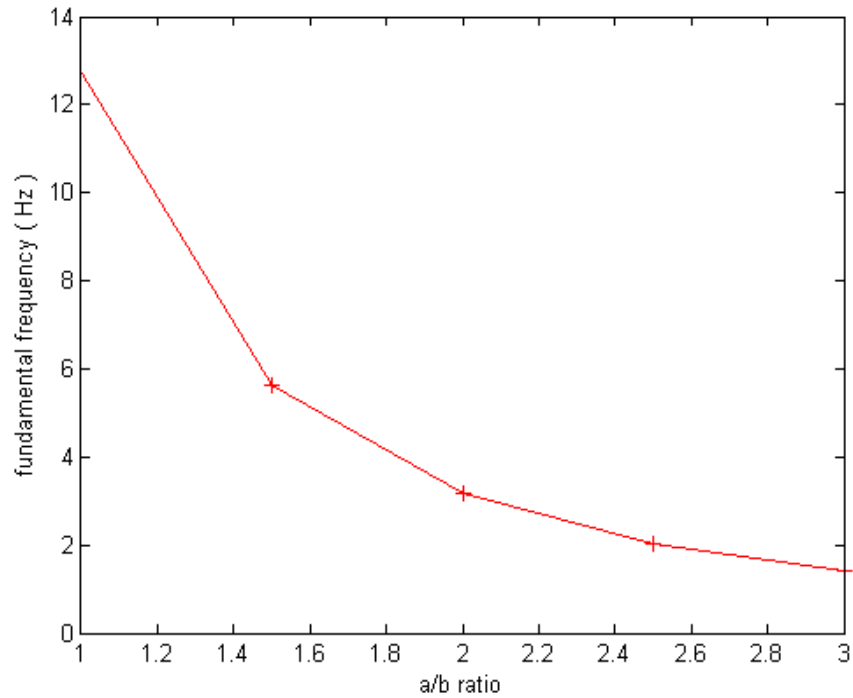
Figure 4.3: Variation of fundamental frequency (ω) with a/b ratio

Table 4.9: Non-dimensional frequencies ($\omega*$) of cantilever Twisted Al/Al_2O_3 FGM plate with varying angle of twist. (n=1,a=1m,a/h=100,a/b=1)

Angle of twist	1st frequency	2nd frequency	3rd frequency	4th frequency
0	15.56	38.05	95.37	121.72
10	15.55	95.37	105.68	143.05
20	15.46	91.89	180.95	189.23
30	15.31	86.06	232.86	236.15
45	15.00	75.66	240.72	282.42

38

are observed with increase in gradient index. The gradient index is varied from 0 to 100. The change in non-dimensional frequencies are observed to be a cubic variation with gradient index. For gradient index 0 to 5 the variation is high and for higher gradient index, variation is less. The observations are given in Table 4.10. The variation of fundamental non-dimensional frequency with gradient index is shown in Figure 4.4

Table 4.10: Non-dimensional frequencies ($\omega*$) of cantilever Twisted Al/Al_2O_3 FGM plate with varying gradient index. (a=1m,a/h=100,a/b=1, $\phi = 20^0$)

Gradient index	1st frequency	2nd frequency	3rd frequency	4th frequency
0	20.24	120.21	222.09	236.33
0.5	17.20	102.23	196.85	207.01
1	15.46	91.89	180.95	189.23
2	14.03	83.35	163.58	171.20
5	13.26	78.73	144.23	153.87
10	12.78	75.87	132.89	143.93
20	11.97	71.05	123.99	134.49
30	11.42	67.84	119.91	129.47
100	10.35	61.51	113.31	120.68

The effect of side to thickness ratio on the free vibration of cantilever pretwisted Al/Al_2O_3 FGM plates is studied. Twisted square plate with angle of twist 15^0 and gradient index =1 is taken for this study. The first four natural frequencies are observed with increase in side to thickness ratio. Table 4.11 shows the variation in natural frequencies with varying side to thickness ratio. From the results, it is observed that the frequency of vibration decreases with an increase in side to thickness ratio. This study is repeated with changing gradient index. The figure 4.5 shows the change in natural frequencies with side to thickness ratio for different gradient indices.
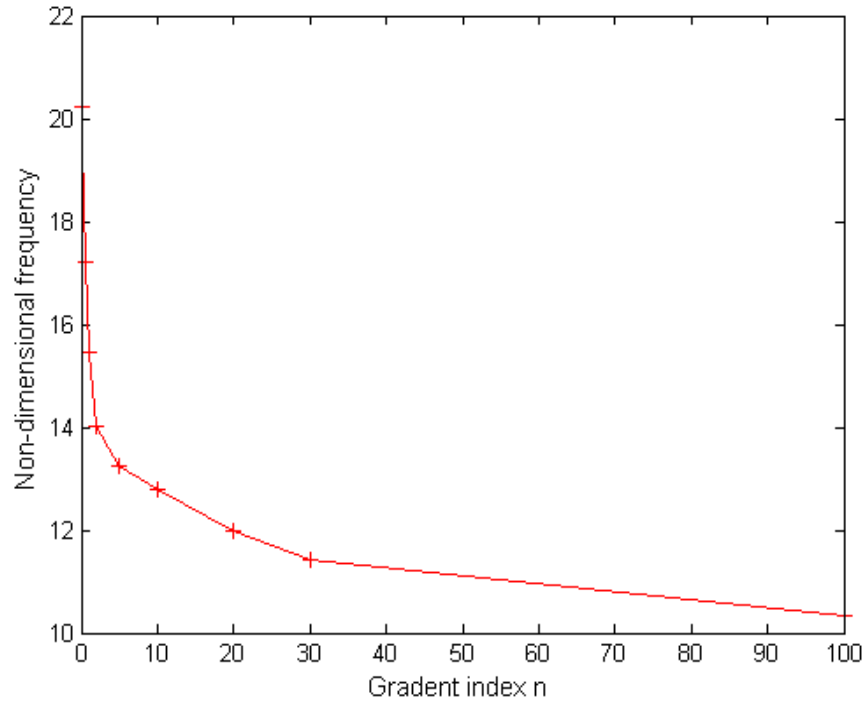
Figure 4.4: Variation of Non-dimensional frequency (ω) with material gradient index

Table 4.11: Natural frequencies (ω) of cantilever Twisted Al/Al_2O_3 FGM plate with varying a/h ratio. (n=1,a=1m,a/h=100,a/b=1, $\phi = 15^0$)

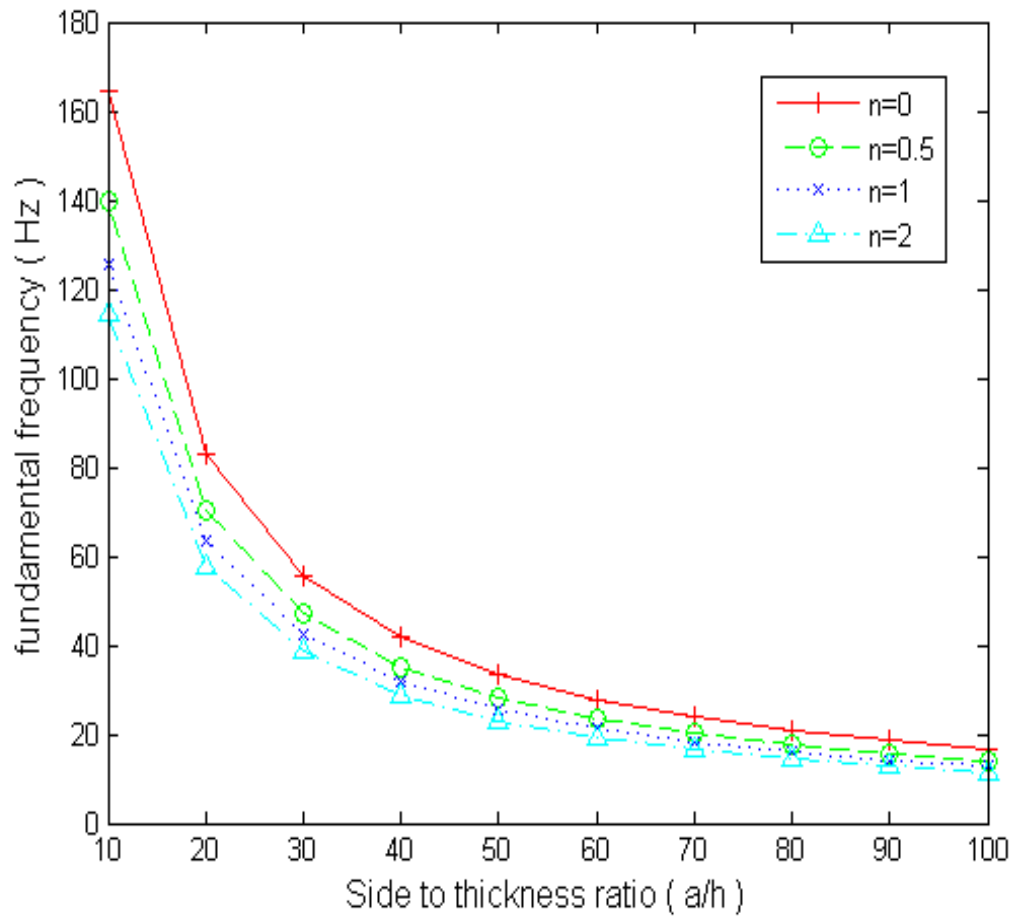| a/h ratio	1st frequency	2nd frequency	3rd frequency	4th frequency
10	125.73	323.30	704.34	878.73
20	63.33	199.76	376.60	491.98
30	42.29	164.25	254.01	339.15
40	31.74	149.13	191.52	263.10
50	25.41	141.02	153.73	218.58
60	21.18	128.42	135.87	189.86
70	18.16	110.29	132.11	170.13
80	15.90	96.65	129.07	155.92
90	14.14	86.19	126.39	145.31
100	12.73	77.49	123.92	137.16

Figure 4.5: Variation of fundamental frequency (ω) with a/h ratio

4.5   Free vibration analysis in thermal environment

The FGM plates are often used in situations where it is exposed to high temperature environment. Due to the inhomogeneous property of FGM plates the temperature change along the thickness is not constant. Through thickness nonlinear temperature variation is considered in this portion. The gradient index and coefficient of thermal conductivity are the determining factors in the temperature change along the thickness.

The influence of temperature stress in the free vibration of pretwisted FGM plate is studied. The FGM plate made up of Silicon Nitride and Stainless steel ($Si_3N_4/SUS304$) is taken for the study. Temperature dependent material properties are considered. Young's modulus and thermal expansion coefficient are considered as temperature dependent. Material properties of different ceramic and metal are given in table 4.6. Temperature dependent coefficients of these materials are given in Table 4.5.
Figure 4.6 shows the nonlinear temperature variation in the thickness direction for different gradient index. The Al/ZrO_2 plate is considered, the temperature at the ceramic surface is kept 600K and metal surface temperature is kept at 300K.

The influence of increase in temperature on the free vibration is studied by increasing the temperature at ceramic face and frequencies are found out at each increase in temperature. The $Si_3N_4/SUS304$ FGM plate is considered in the study and temperature is given at Si_3N_4 face. The cantilever plate with gradient index = 1 is considered for the study. The first three natural frequency parameters are compared with an increase in temperature. The temperature at the metal surface is kept constant.Table 4.12 gives first three natural frequency parameters (Ω) for $Si_3N_4/SUS304$ FGM plate for change in ceramic temperature. From the study it is observed that the thermal initial stress decreases the natural frequency of vibration.
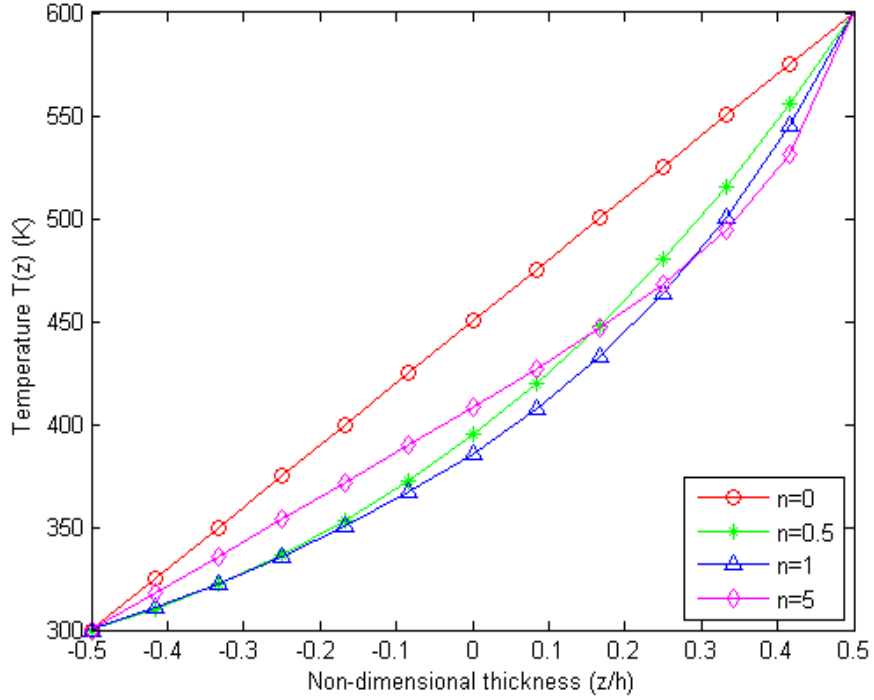
42

Figure 4.6: Through thickness temperature variation of Al/ZrO_2 FGM plate

Table 4.12: Natural frequencies (ω) of cantilever Twisted $Si_3N_4/SUS304$ FGM plate with varying temperature. (a/h=10, n=1, a/b=1, $\phi = 20^0$)

Temperature (K)	Mode 1	Mode 2	Mode 3	Mode 4
Tc=300, Tm=300	1.3748	3.7147	7.3448	9.4530
Tc=325, Tm=300	1.3160	3.6444	7.2876	9.3892
Tc=350, Tm=300	1.2527	3.5716	7.2285	9.2334
Tc=375, Tm=300	1.1842	3.4961	7.1675	9.2554
Tc=400, Tm=300	1.1096	3.4178	7.1045	9.1851
Tc=425, Tm=300	1.0272	3.3364	7.0394	9.1125
Tc=450, Tm=300	0.9350	3.2518	6.9720	9.0378

43

The influence of gradient index in the case of temperature depended free vibration is studied. For different gradient index the natural frequency parameter is found out with an increase in temperature at ceramic face. Table 4.13 gives natural frequency parameter (Ω) for $Si_3N_4/SUS304$ FGM plate for change in temperature and gradient index. The Figure 4.7 shows this variation graphically.

Table 4.13: Natural frequencies (ω) of cantilever Twisted $Si_3N_4/SUS304$ FGM plate with varying temperature and gradient index. (a/h=10, a/b=1, $\phi = 20^0$)

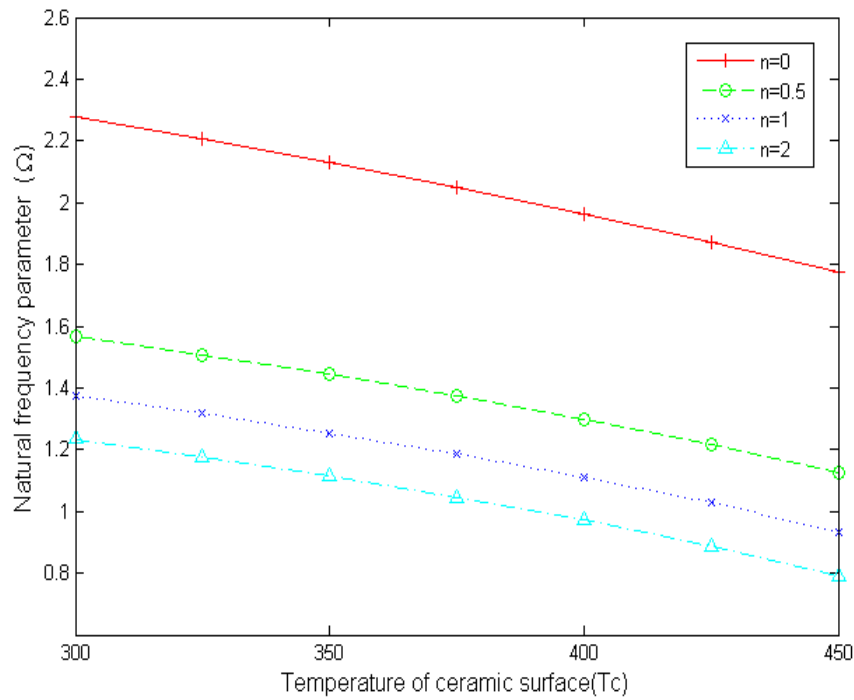| Temperature (K)	n=0	n=0.5	n=1	n=2
Tc=300, Tm=300	2.2782	1.5688	1.3748	1.2348
Tc=325, Tm=300	2.2066	1.5079	1.3160	1.1769
Tc=350, Tm=300	2.1310	1.4429	1.2527	1.1143
Tc=375, Tm=300	2.0508	1.3731	1.1842	1.0460
Tc=400, Tm=300	1.9652	1.2975	1.1096	0.9707
Tc=425, Tm=300	1.8737	1.2152	1.0272	0.8866
Tc=450, Tm=300	1.7750	1.1244	0.9350	0.7908

Figure 4.7: Variation of natural frequency parameter with temperature

The influence of temperature in free vibration of cantilever pretwisted plate with different side to thickness ratio is studied. Table 4.14 gives the variation in fundamental frequency of $Si_3N_4/SUS304$ FGM plate with temperature of ceramic surface for different side to thickness ratio. Figure 4.8 shows the variation of fundamental frequency with temperature. From the figure for higher side to thickness ratio the variation in natural frequency with temperature is not linear.

Table 4.14: Natural frequencies (ω) of cantilever Twisted $Si_3N_4/SUS304$ FGM plate with varying temperature and a/h ratio. (n=1, a/b=1, $\phi = 20^0$)

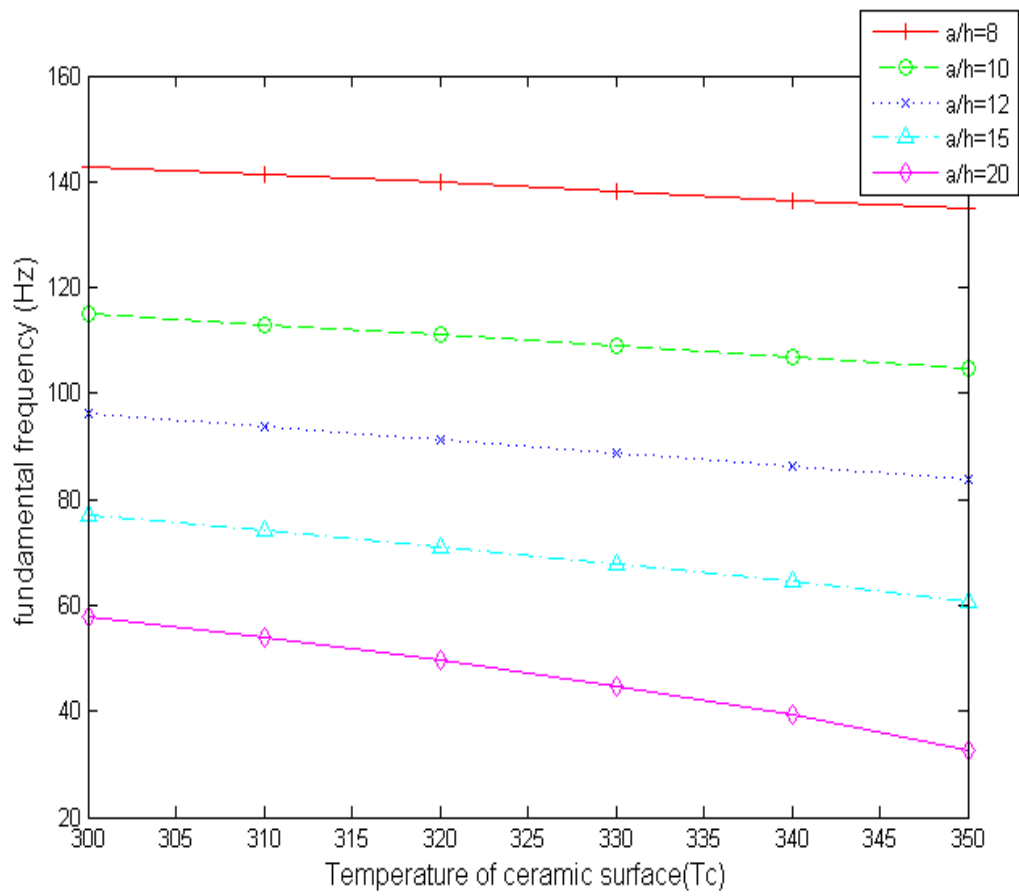| Temperature (K)	a/h=8	a/h=10	a/h=12	a/h=15	a/h=20
Tc=300, Tm=300	142.94	114.97	96.11	77.09	57.95
Tc=310, Tm=300	141.38	113.05	93.80	74.20	54.04
Tc=320, Tm=300	139.79	111.06	91.41	71.14	49.72
Tc=330, Tm=300	138.17	109.02	88.92	67.90	44.86
Tc=340, Tm=300	136.52	106.92	86.32	64.43	39.25
Tc=350, Tm=300	134.83	104.76	83.61	60.70	32.49

Figure 4.8: Variation of fundamental frequency with temperature

Chapter 5

CONCLUSIONS

Chapter 5

Conclusion

5.1 Conclusion

From the free vibration analysis of cantilever twisted FGM plates following conclusions are made in this study.

1. With the increase in the angle of pretwist, the fundamental frequency of vibration decreases.

2. As the gradient index increases, the fundamental frequency of vibration decreases.

3. The fundamental frequency of vibration decreases as the aspect ratio (a/b) increases.

4. The fundamental frequency of vibration decreases as the length to thickness ratio (a/h) increases.

5. The natural frequencies of vibration of FGM plate decreases with increase in temperature gradient due to reduction of stiffness.

6. The reduction in natural frequency due to temperature need not be linear, it depends upon side to thickness ratio and gradient index.

5.2   Future Work

Present study considered the FGM plate as step wise graded and the material properties are varied accordingly. In the actual case the material properties are varying gradually, if the gradual variation in material properties are taken in to account the results will be more accurate. In this study free vibration analysis is done, dynamic studies and the effect of lateral load is a scope for further study. The study can be extended to sandwich FGM plates and FGM plates with change in porosity.

Bibliography

[1] Aboudi, J., Pindera, M. J., Arnold, S. M. "Higher order theory for functionally graded materials," *Composites: Part B*, 30, (1999): 777-832.

[2] Alibakhshi, R. and Khavvaji, A. "Free vibration analysis of thick functionally graded rectangular plates using variable refined plate theory," *Journal of Mechanical Research and Application*, 3, no. 1 (2011): 65-73.

[3] Baferani, A. H., Saidi, A. R., and Jomehzadeh, E. "An exact solution for free vibration of thin functionally graded rectangular plates" *Journal of Mechanical Engineering Science* , 225, Part C (2010):

[4] Baferani, A. H., Saidi, A. R., and Jomehzadeh, E. "Exact analytical solution for free vibration of functionally graded thin annular sector plates resting on elastic foundation," *Journal of Vibration and Control*,18, no. 2 (2011): 246-267.

[5] Biner, S. B. "Thermo-elastic analysis of functionally graded materials using Voronoi elements," *Materials Science and Engineering*,A315, (2001): 136-146.

[6] Chandrashekhara, K. "Free vibrations of anisotropic laminated doubly curved shells," *Computers and Structures*,33, no.2 (1989): 435-440.

[7] Cho, J. R. and Ha, D. Y. "Averaging and finite element discretization approaches in the numerical analysis of functionally graded materials, "*Materials Science and Engineering*,A302, (2001): 187-196.

[8] Dong, C. Y. "Three dimensional free vibration analysis of functionally graded annular plates using the ChebyshevRitz method," *Materials and Design*,29 (2008): 1518-1525.

[9] Fallah, A., Aghdam, M. M. and Kargarnovin, M. H. "Free vibration analysis of moderately thick functionally graded plates on elastic foundation using the extended Kantorovich method," *Arch Appl Mech*,83, (2013): 177-191.

[10] Huang, X. L. and Shen, H. S. "Nonliear vibration and dynamic response of functionally graded plates in thermal environments," *International Journal of Solids and Structures*, 41, (2004): 2403-2427.

[11] Kee, Y.J. and Kim, J.H. "Vibration characteristics of initially twisted rotating shell type composite blades," *Composite Structures*, 64, no. 2 (2004): 151-159.

[12] Kiani, Y., Eslami, M. R. "An exact solution for thermal buckling of annular FGM plates on an elastic medium," *Composites: Part B*, 45, (2013): 101-110.

[13] Malekzadeh, P., Shahpari, S. A., Ziaee, H. R. "Three-dimensional free vibration of thick functionally graded annular plates in thermal environment," *Journal of Sound and Vibration*, 329, (2010): 425-442.

[14] Nabi, Y.J. and Ganesan, N. "Comparison of beam and plate theories for free vibrations of metal matrix composite pretwisted blades," *Journal of Sound and Vibration*, 189, no. 2 (1996): 149-160.

[15] Noda, N. "Thermal stresses in functionally graded materials," *Journal of Thermal Stresses*, 22, (1999): 477-512.

[16] Rath, M. K. and Sahu, S. K. "Vibration of woven fiber laminated composite plates in hygrothermal environment," *Journal of Vibration and Control*, 18, no. 2, (2011): 1957-1970.

[17] Reddy, J. N. "Analysis of functionally graded plates," *International Journal for Numerical Methods in Engineering* , 47, (2000): 663-684.

[18] Reddy, J. N. and Cheng, Z. Q. "Three-dimensional thermomechanical deformations of functionally graded rectangular plates,"*Eur. J. Mech. A/Solids* 20, (2001): 841-855.

[19] Reddy, J. N. and Chin, C. D. "Thermomechanical analysis of functionally graded cylinders and plates," *Journal of Thermal Stresses*, 21, no. 6, (1998): 593-626.

[20] Sahu, S.K., and Datta, P.K. "TDynamic instability of laminated composite rectangular plates subjected to non-uniform harmonic in-plane edge loading," *Journal of Aerospace Engineering*, 214, Part G, (2000): 295-312.

[21] Singha, M. K., Prakash, T., Ganapathi, M. "Finite element analysis of functionally graded plates under transverse load," *Finite Elements in Analysis and Design*, 47, (2011): 453-460.

[22] Schmauder, S., Weber, U. "Modeling of functionally graded materials by numerical homogenization," *Archive of applied mechanics*, 71, no. (2001): 182-192.

[23] Shen, H. S. "Nonlinear bending response of functionally graded plates subjected to transverse loads and in thermal environments," *International Journal of Mechanical Sciences*, 44, (2002): 561-584.

[24] Shen, H. S., Zheng, J. J. and Huang, X. L."The effects of hygrothermal conditions on the dynamic response of shear deformable laminated plates resting on elastic foundations," *Journal of reinforced plastics and composites*, 23, no. 10 (2013): .

[25] Srinivas, G., Sivaprasad, U. "Simulation of traditional composites under mechanical loads," *International Journal of systems, Algorithms Application*, 2, (2012):

[26] Suresh Kumar, J., Reddy, B. S., Reddy, C. E. "Nonlinear bending analysis of functionally graded plates using higher order theory," *International*

Journal of Engineering Science and Technology, 3, (2011):

[27] Thai, H. T., Choi, D. H. "Size dependent functionally graded Kirchhoff and Mindlin plate models based on a modified couple stress theory," *Composite Structures*, 95, (2013): 142-153.

[28] Wattanasakulpong, N. "Thermal buckling and elastic vibration analysis of functionally graded beams and plates using improved third order shear deformation theory," *School of Mechanical and Manufacturing Engineering, The University of New South Wales*, (2012):

[29] Wetherhold, R. C., Seelman, S., Wang, J. "The use of functionally graded materials to eliminate or control thermal deformation," *Composites Science and Technology*, 56, (1996): 1099-1104.

[30] Yin, S., Yu, T. and Liu, P. "Free Vibration Analyses of FGM Thin Plates by Isogeometric Analysis Based on Classical Plate Theory and Physical Neutral Surface," *Advances in Mechanical Engineering*, (2013):

[31] Zhao, X., Lee, Y. Y., Liew, K. M. "Free vibration analysis of functionally graded plates using the element-free kp-Ritz method," *Journal of Sound and Vibration*, 319, (2009): 918-939.